Comparative Multi-Objective Assessment of Shared and Standalone Rooftop PV-Battery Systems for Energy Autonomy and Infrastructure Efficiency

Nishchaya Kumar Mishra[1], Sameer Patel[1, 2, 3, *]

[1]Department of Civil Engineering, [2]Department of Chemical Engineering, [3]Kiran C. Patel Centre of Sustainable Development, Indian Institute of Technology Gandhinagar, Palaj, Gandhinagar, Gujarat 382355, India

Abstract

Energy autonomy and energy security are becoming increasingly critical in modern urban energy systems. In this context, photovoltaic (PV)-battery systems offer a promising pathway to increase renewable energy utilization and reduce dependence on centralized electricity networks. This study presents a comparative multi-objective optimization framework for evaluating standalone- and shared PV-battery systems for residential energy applications. The optimization simultaneously considers PV reliance, panel area, battery storage, lifetime cost, payback period, and carbon emission mitigation under varying objective-weight combinations. The results demonstrate that shared integration substantially improves infrastructure utilization and economic feasibility compared to standalone household systems optimized independently. Across all weight combinations, the shared system reduced per-household panel area requirements by 61 ± 42 % and 81 ± 12 %, while simultaneously decreasing lifetime cost and payback period by 64 ± 38 % and 22 ± 12 %, respectively. Although the shared system exhibited lower PV reliance and carbon mitigation potential, the significant reductions in infrastructure and economic burdens highlight the advantages of shared energy and storage at the community level. Overall, the findings reinforce the importance of cooperative renewable-energy systems in improving energy accessibility, affordability, and long-term energy equity.

Keywords

PV-battery integration, shared energy systems, multi-objective optimization, energy security

1. Introduction

More than 80% of global energy comes from fossil fuels and their derivatives [1], wherein buildings account for over one-third of global energy resources [2] and are responsible for ~37% of global energy and process-related carbon emissions [3], contributing to adverse climate effects. In the past three decades (1990-2019), global CO_2 emissions from buildings increased by ~50% [4], and operational energy use has increased at an average annual rate of 1% over the past decade [4]. In the coming decades, as demand for buildings increases, the construction sector is expected to grow faster than the services and manufacturing sectors. Since the energy intensity of buildings and building performance have remained constant in the past few years [2], the total energy consumption and carbon emissions from buildings are bound to increase. This suggests a causal relationship between buildings and climate change, where buildings contribute to climate change, which in turn influences energy consumption. Simultaneously, an energy penalty is incurred to maintain healthy, comfortable indoor environments, further highlighting the energy intensity of buildings [5–7]. This additional energy demand will increase grid load and carbon emissions, as fossil-fuel-based generation still accounts for a significant share of global energy demand.

Recent research and policies have advocated for net-zero or nearly zero-energy buildings [8–13]. The concept of zero-energy buildings can be expanded to create nearly zero-energy communities, where the community becomes energy self-sufficient. Moreover, integrating renewable energy sources at the community and household levels could help ensure energy equity and alleviate energy poverty worldwide, while promoting multiple Sustainable Development Goals (SDGs) [14,15]. Joshi et al. [16] analyzed 130 million km^2 of global land surface area to demarcate 0.2 million km^2 of rooftop area and reported a potential annual electricity generation of 27 PWh (petawatt-hours). This potential for electricity generation from rooftop solar photovoltaic (PV) is significant, as total electricity use in all homes worldwide was only ~6 PWh in 2019 [17,18].

While realizing this potential would depend on the development and cost of solutions to store the generated energy, incorporating solar PV into the energy mix is imperative to reduce energy-derived carbon emissions and advance multiple SDGs. However, a temporal mismatch exists between solar PV system output and residential electricity demand, which is a primary reason for the low adoption of residential PV systems, along with initial investment and trade-offs between reliance and cost [19–22]. Another challenge is optimizing the size of the PV system and battery storage capacity to realize the potential of solar energy while minimizing cost and space utilization. Studies have proposed different strategies for designing and optimizing solar PV size and storage capacity based on various metrics [23–27]. O'Shaughnessy et al. [26] used a mixed-integer linear programming model to minimize life-cycle energy costs for a residential household. The study reported that an integrated approach to PV optimization, utilizing batteries and load control devices, improved customer economics compared to standalone solar. Further, the economics of solar PV systems depend on the grid export rates. Khanal et al. [25] studied the effects of energy sharing and electricity tariffs on the optimal sizing of PV and storage for grid-connected houses. The study design involved energy sharing between two houses (one with PV and storage, and the other without) at a mutually agreed-upon price, while minimizing the cost of electricity for both houses. Similarly, other studies have defined objective functions to minimize individual or multiple components, such as the levelized cost of electricity, PV reliance, and environmental cost [28–31]. However, few studies have simultaneously considered dynamic grid export rates, life-cycle costs, and direct environmental costs to optimize the size and battery capacity.

Transitioning to low-carbon, energy-efficient buildings is essential not only for climate mitigation but also for ensuring long-term energy autonomy, energy security, and sustainable urban development. Therefore, this work develops a multi-objective optimization framework to design and compare standalone- and shared PV-battery systems using real residential electricity consumption data. An energy management system (EMS) model is developed to regulate grid export, battery operation, and electricity utilization. The framework simultaneously evaluates PV reliance, lifetime cost, payback period, and direct carbon mitigation to determine optimal PV and battery configurations. The proposed framework enables a systematic understanding of the trade-offs between technical performance, economic feasibility, and environmental benefits across different optimization objectives. Finally, the study investigates how shared systems improve infrastructure utilization, economic feasibility, and system robustness relative to independently optimized household systems, while advancing energy sufficiency, enhancing energy autonomy and security, and promoting equitable access to clean and affordable energy.

2. Methodology

2.1 Energy Management System Model

The energy consumption profiles and statistics for households are presented in Fig. S1 and Table S1 of Section S1 in the Supplementary Information (SI). A grid-connected solar PV-storage system has been modelled to meet the energy demand of the selected households in this work, whose energy flow diagram is shown in Fig. 1. The system consists of a charge controller for extracting maximum power from the PV and controlling battery charging and discharging, and a DC/AC inverter is integrated to transform the DC power from PV arrays and battery bank to AC power. An energy balance model, governed by a rule-based algorithm, controls the energy flow from PV arrays to the battery bank, home, and grid export. According to the energy balance model (Fig. 2), the energy generated initially charges the battery bank. The excess energy is converted to AC power to meet the home's demand, and any surplus is exported to the grid. The proposed rule-based algorithm reduces the grid dependency of homes to meet the energy demand. In the developed energy flow model, the charge controller prioritizes battery charging if the battery is not fully charged whenever solar energy is available (Fig. 2A). The home demand is satisfied through combined energy from the PV array and battery bank (Fig. 2A), and the deficit is taken from the grid (Fig. 2C).

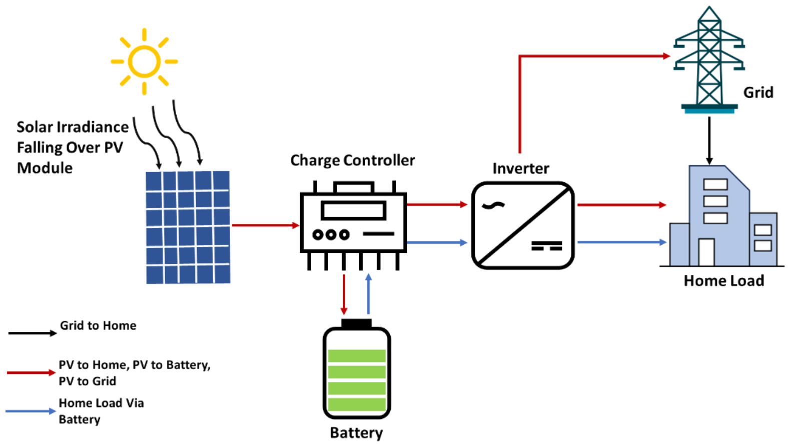

Figure 1. Schematic of energy generation and management of a grid-connected solar PV-storage system.

Intermittent charging and discharging of the battery can be used to estimate the battery's storage cycle. The capacity of a battery reduces with the number of battery cycles, and multiple studies have investigated the relationship between battery retention capacity and the total number of battery storage cycles [32–36]. A simplified model for battery capacity variation with battery cycle has been adopted from [36] and is discussed in Section S2.

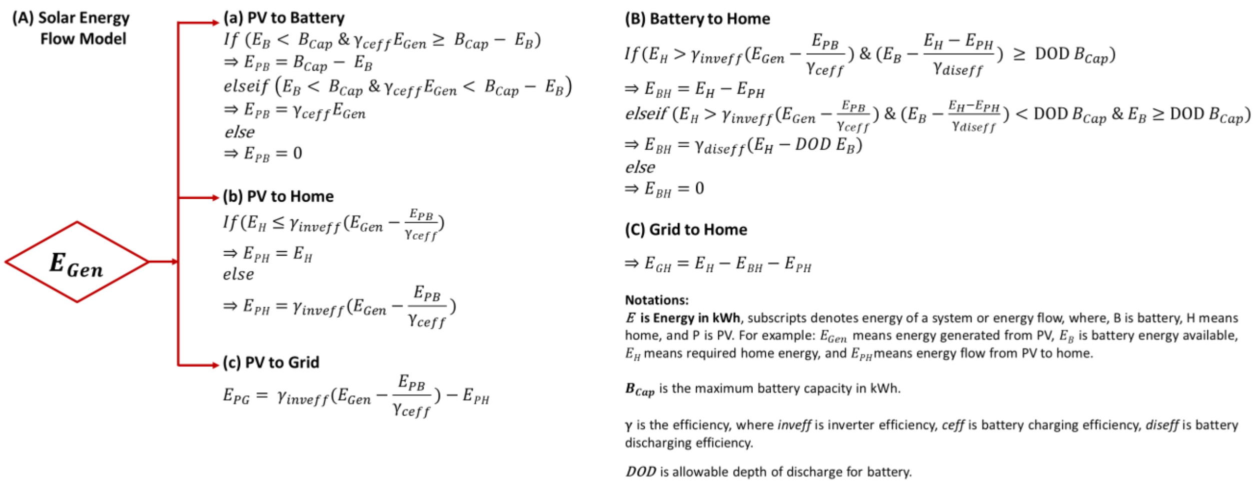

Figure 2. Rule-based algorithm for (A) solar energy flow to charge the battery, meet home demand and grid export, (B) battery discharging, and (C) grid import

2.2 Objectives and Cost Function

This study aims to develop an optimization strategy for sizing PV arrays and storage capacity for a shared PV-battery system. It performs a comparative analysis of standalone and shared systems. The objectives of the optimization are to minimize the lifetime cost of the system, the payback period, and direct carbon emissions due to grid electricity usage, while maximizing the reliance on the PV system to meet the load demand. The formulation of the multi-objective optimization problem needs models to estimate the individual objectives, which are discussed below.

2.2.1 Lifetime Cost and Payback Period

The lifetime cost estimate has been calculated for a panel life of 30 years. Since the life of different components may be less than the panel life, replacement of those components has been considered. The inflation and discount rates have also been included to account for the change in the value of money over time. The lifecycle of various components and their corresponding market prices in India are compiled in Table 1. All prices and costs are converted to US dollars, assuming an exchange rate of one US dollar is equivalent to 100 Indian rupees.

Table 1. Typical components of a battery-integrated PV system with their prices in the Indian market. Data has been obtained from multiple online sellers. MPPT: Maximum Power Point Tracking.

Component	Market Price (USD*)	Lifetime[e]
PV Panel	0.438[a]	30 years
Battery	100.01[b]	8000 cycles
MPPT	120.01-420.012[c]	15 years
Grid-tie Inverter	80.01[d]	15 years

[a]per Watts, [b]per kWh for 24V LFP battery, [c]depending upon the maximum current, [d]per kW, Conversion rate: 1 USD = ₹100, [e]as per the prevalent market information

Afterward, the total investment for the battery-integrated solar PV system is calculated based on the lifecycle cost of various components. The method for estimating the number of replacements, lifecycle cost, and total investment is shown in Eq. (1).

$$N_{replacements} = \left\lceil \frac{Panel_T}{T_C} - 1 \right\rceil, where\ \lceil x \rceil = \min\{n \in \mathbb{Z} : n \geq x\}$$

$$IC_{component} = N_{components}\ x\ Per\ Unit\ Cost$$

$$LC_{component} = \sum_{i=0}^{N_{replacements}} IC_{component}\ x\ \frac{(1+IR)^{i\,T_C}}{(1+DR)^{i\,T_C}}$$

Eq. (1)

where, $N_{replacements}$ means the number of replacements during the panel life, $Panel_T$ is the panel life in years, T_C is the component life in years, $IC_{component}$ is the initial investment cost, $N_{components}$ means the number of individual components initially installed, $LC_{component}$ represents the lifetime cost of the component. *IR* and *DR* are the inflation and discount rates, respectively.

Unlike other components, which are assumed to have a constant lifetime regardless of usage pattern, battery life is measured in terms of the number of charge-discharge cycles. Therefore, Eq. (2) is used to estimate the total life cycle of the battery.

$$T_{battery} = \frac{Total_{cycle}}{N_{cycle}(in\ one\ year)}$$

Eq. (2)

where, $T_{battery}$ is the number of years after which the battery needs to be replaced, which is obtained as the ratio of total battery storage cycle ($Total_{cycle}$) and the number of battery cycles in one year (N_{cycle}). $N_{battery\_replacements}$ is the number of replacements needed over the panel life, and other notations have the same meanings as discussed above. The total lifetime investment of the complete system is further calculated as the sum of the costs of the individual components. The investment estimate here does not account for subsidies provided by various government schemes.

The system's payback period depends on the lifetime cost, revenue generated from grid exports, and the offset energy cost of the home energy demand satisfied by the system. The offset energy cost of the home demand adds to the revenue generated by the system, which is later used to estimate the payback period. Further, it also represents the degree of reliance on the designed PV system. The grid export prices are dynamic and have been obtained from the India Energy Exchange at 15-minute resolution [37]. The annual revenue from energy exports (R_{grid_export}) and the offset energy cost ($Cost_{offset}$) have been estimated, as shown in Eq. (3).

$$R_{grid\_export} = \sum SP\ x\ E_{PG}$$

$$Cost_{offset} = \sum CP\ x\ (E_{PH} + E_{BH})$$

Eq. (3)

R_{grid_export} is calculated annually as the sum of the product of the electricity selling price (SP) and grid electricity export (E_{PG}). CP is the cost of the electricity bought from the grid. E_{PH} and E_{BH} are the energy flows from PV and battery to the home. The total revenue from the system is adjusted for the panel's lifetime by including *IR* and *DR*. The break-even year, when cumulative revenue exceeds the total investment for distinct combinations of panel area and battery capacity, is considered the payback period.

2.2.2 Direct Carbon Emissions Mitigated

India still heavily relies on fossil fuel-based sources for electricity generation, with ~53% of its installed power capacity based on coal and natural gas derivatives as of 2024 [38]. This dependency on fossil fuel-derived resources results in carbon emissions. The Central Electricity Authority (CEA) of India publishes the annual average carbon emission factor of the Indian grid, accounting for renewable energy sources. For 2023-24, the average carbon emission for grid electricity is 0.727 kg CO_2/kWh, demonstrating an increasing trend over the last few years (0.703 in 2020-21, 0.715 in 2021-22, and 0.716 in 2022-23) [39]. In 2022-23, domestic consumers, primarily households, accounted for ~28% of total electricity consumption in India [40]. This reliance of domestic consumers on the grid (~$4x10^5$ GWh in 2023-24) [40] and the significant carbon intensity of grid electricity resulted in more than 250 million tons of CO_2 emissions in 2023-24. One way to reduce the direct carbon emissions associated with building electricity consumption is to adopt on-site solar PV systems, which have been designed and discussed in this work. Given that total building energy consumption is expected to grow, reducing reliance on fossil-fuel-derived electricity and integrating renewables into the electricity supply chain are imperative. Therefore, the optimization problem formulated in this work includes direct annual carbon emissions mitigated by solar energy generation as one of the objectives of the cost function. The grid export, along with home demand met directly by solar energy and via battery storage, has been included in the calculation of avoided carbon emissions, as these sources have zero direct carbon emissions and ultimately reduce the carbon footprint of both the building's energy and the grid. The total annual carbon emissions avoided by installing PV arrays are estimated using Eq. (4).

$$CO_2\ emissions\ avoided = \sum (E_{PH} + E_{PG} + E_{BH})\ x\ EF_{grid}$$

Eq. (4)

where EF_{grid} is the carbon emission factor of the grid electricity in kg CO_2/kWh. E_{PH}, E_{PG}, and E_{BH} represent the energy flows from PV to the home, from PV to the grid, and from the battery to the home, respectively.

2.2.3 Reliance of the PV-Battery System

A battery-integrated PV system provides a more reliable energy source, given that grid intermittency remains a challenge in many Indian states. The reliability of the system directly depends on the size of the PV system and the battery storage capacity. With a large area of the PV system, the energy generated is greater, while a larger battery bank ensures an uninterrupted energy supply during grid unavailability and nighttime. However, poorly sized PV-battery systems may not provide the required reliability and return on investment. Therefore, designing and operating an optimally sized PV-battery system is crucial to ensure sufficient reliability while minimizing costs. Thus, the reliance on the PV-battery system to meet the home load demand needs to be assessed and has been included in the cost function. Subsequently, the reliance has been estimated based on the fraction of home load demand fulfilled directly (E_{PH}) and indirectly (E_{BH}) through the PV-generated energy.

2.2.4 Multi-objective Optimization and Cost Function

The various aspects of the PV-battery system modeled above have been used to formulate a cost function that concurrently optimizes different objectives (payback period, lifetime cost, carbon mitigation, and reliance) and has been defined as shown in Eq. (5). The individual objectives have been normalized to ensure that they remain within a comparable range (0-1) with each other to avoid inherent dominance of any objective. An objective-wise normalization factor has been adopted where the payback period has been normalized by 30 (lifespan of the PV module), cost and annual carbon emissions avoided have been normalized by the maximum cost and the maximum annual carbon emissions avoided of all possible combinations of PV size and battery capacity, and the reliance remains as a fraction that ranges between zero and one where one means 100% reliance. Eq. (5) represents a weighted combination of these objectives.

$$minimize$$

$$obj = -W_1 Reliance - W_2 \frac{CO_2\ emissions\ avoided}{\max(CO_2\ emissions\ avoided)} + W_3 \frac{PP}{30} + W_4 \frac{\sum_{i \in components} LC_i}{\max(\sum_{i \in components} LC_i)}$$

Subjected to

$$\mathrm{PV}_{sizemin} \leq \mathrm{PV}_{size} \leq \mathrm{PV}_{sizemax}$$

$$\mathrm{Battey}_{capacitymin} \leq \mathrm{Battery}_{capacity} \leq \mathrm{Battery}_{capacitymax}$$

Eq. (5)

W_1, W_2, W_3, and W_4 are the relative weights assigned to different objectives in the cost function, PP is the payback period in years, and LC_i is the lifetime cost of component i. The PV module size (in m^2) and battery capacity (in kWh) vary from $PV_{sizemin}$ (1.955 m^2 for both standalone- and shared systems) to $PV_{sizemax}$ (389.045 m^2 for standalone and 3892.405 m^2 for shared systems), and from $Battery_{capacitymin}$ (0 kWh for both standalone- and shared systems) to $Battery_{capacitymax}$ (50 kWh for standalone and 200 kWh for shared systems), respectively.

3. Results and Discussion

3.1 Sensitivity Analysis of Objectives at Different Weightages

The multi-objective optimization formulated in Eq. (5) is essential for the design and operation of distributed PV systems, as system performance is governed by several conflicting objectives that cannot be simultaneously optimized. For example, increasing PV reliance and reducing emissions often requires larger panel areas and battery storage, which, in turn, increase investment costs and may adversely affect economic indicators. To obtain optimal solutions of Eq. (5), a weighted-sum method that balances competing objectives by assigning relative weights is employed in this study. This framework enables the generation of a wide range of feasible solutions corresponding to different decision-making scenarios. Moreover, it is important to evaluate how variations in objective weights affect the resulting optimal solutions, as stakeholders may prioritize environmental sustainability, economic feasibility, or energy independence differently. Therefore, a weight sensitivity analysis is performed to investigate the influence of prioritizing different optimization objectives on the system design and performance. Figs. 3 and 4 demonstrate the sensitivity of different components in Eq. (5) at varying relative weights assigned to them while designing standalone household-level PV systems and shared PV systems, respectively. Based on the observed trends in the weight-sensitivity analysis, a comparative discussion between standalone and shared systems is presented with respect to variations across different objectives.

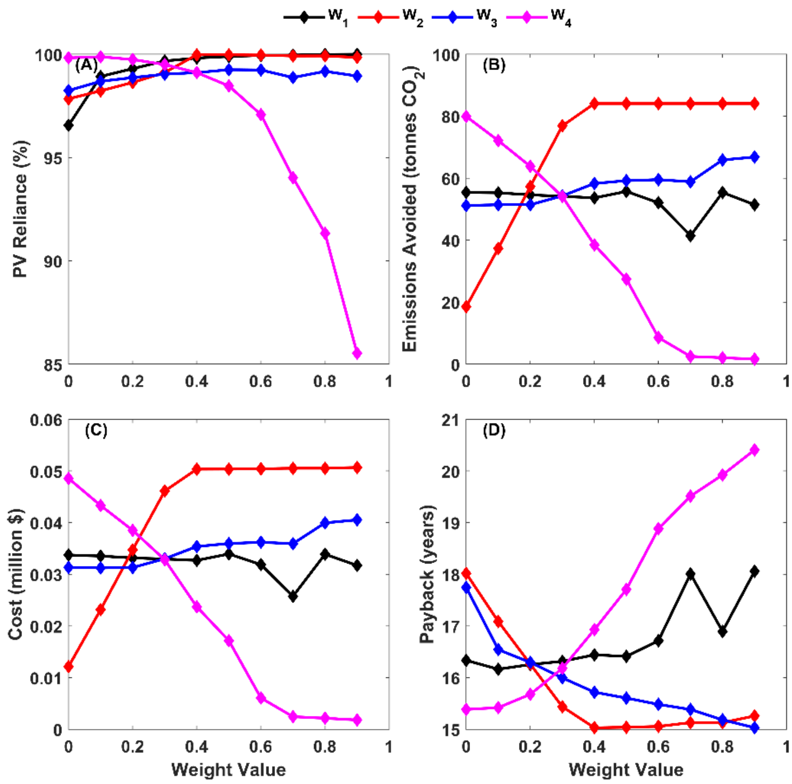

Figure 3. Sensitivity of (A) PV reliance, (B) avoided CO_2 emissions, (C) lifetime investment, and (D) payback period with varying weights (W_1: PV reliance, W_2: CO_2 emissions avoided, W_3: payback period, and W_4: lifetime investment) in the multi-objective cost function for standalone PV systems. Here, the average values across different combinations have been plotted.

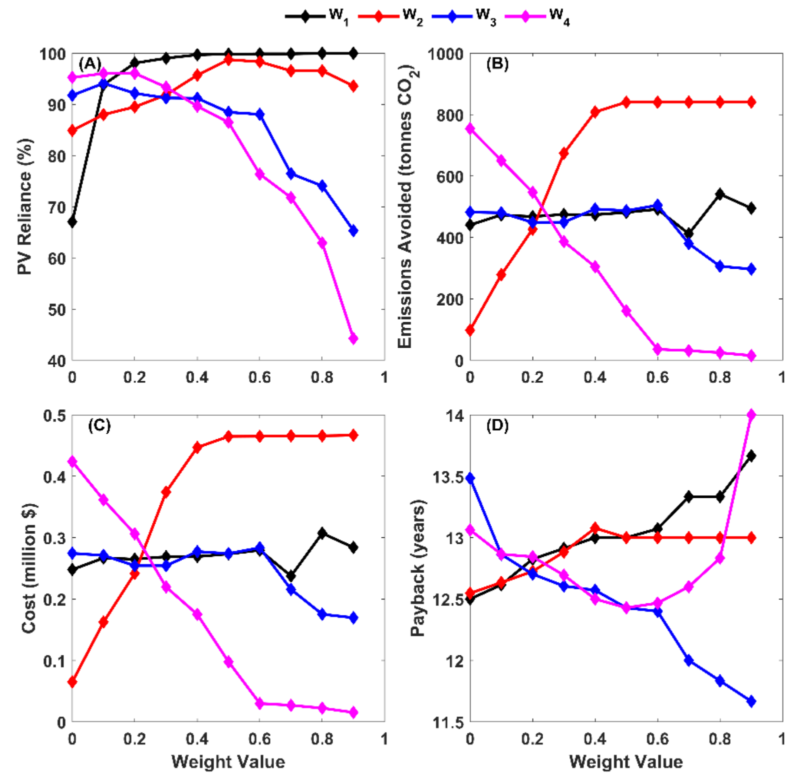

Figure 4. Sensitivity of (A) PV reliance, (B) avoided CO_2 emissions, (C) lifetime investment, and (D) payback period with varying weights (W_1: PV reliance, W_2: CO_2 emissions avoided, W_3: payback period, and W_4: lifetime investment) in the multi-objective cost function for shared PV systems. Here, the average values across different combinations have been plotted.

The reliance on the PV-battery system exhibits distinct trends for the standalone and shared configurations (Fig. 3A and 4A). For both systems, reliance declines with increasing W_4 (the relative weight assigned to lifetime cost), indicating that minimizing cost reduces the achievable energy security from the system. Specifically, the average reliance decreases from approximately 100% to 85% for standalone systems and from approximately 96% to 44% for shared systems as W_4 increases from 0 to 0.9. In contrast, the standalone systems show minimal sensitivity to variations in the remaining weights (W_1, W_2, and W_3), maintaining a high reliance of $98.5 \pm 1.4\%$. However, the shared system demonstrates greater sensitivity to W_3 (the relative weight assigned to the payback period), with reliance decreasing from approximately 92% to 65% as W_3 increases from 0 to 0.9. Since PV reliance is directly determined by the panel area and battery storage capacity, if other parameters are held constant, these trends indicate that minimizing the payback period favors smaller PV-battery configurations, enabling faster economic recovery and break-even for shared-PV-battery systems. For variations in W_1 and W_2, the shared system initially shows a moderate increase in reliance, with a range of 94.5 ± 1.7 %. Overall, the results demonstrate that the shared system is more sensitive to economic objective weighting, highlighting trade-offs between energy autonomy and economic feasibility.

Furthermore, the carbon intensity and the lifetime cost of the standalone and shared systems demonstrate similar responses to variations in objective weights. Both parameters decrease monotonically with increasing W_4 (the relative weight assigned to lifetime cost), whereas increasing W_2 (the relative weight assigned to carbon emissions) results in higher system cost and lower carbon emissions, reflecting trade-offs between environmental performance and economic feasibility. At the same time, the payback period responds differently to variations in weights. While the payback period for the standalone system increases with W_4, the shared system demonstrates a U-shaped profile, indicating the existence of an optimal W_4 value corresponding to a minimum payback period. This behavior suggests that the favorable economic performance at the community scale is achieved when the system cost is constrained within an optimal range. However, imposing stricter cost minimization beyond this point increases the payback period, as it restricts the feasible PV panel and battery storage capacity, thereby reducing energy generation and overall economic returns. The means and deviations in PV reliance, avoided CO_2 emissions, lifetime cost, and payback periods across variations in objective weights are also presented in Table S2.

In brief, the sensitivity analysis highlights the interdependence and trade-offs among the technical, environmental, and economic objectives governing PV-battery system sizing. Increasing the relative importance of economic objectives (lifetime cost and payback period) favors smaller PV-battery configurations, thereby reducing PV reliance and the potential for emissions mitigation. Contrarily, prioritizing environmental objectives promotes larger systems with higher reliance and lower carbon intensity, though at higher investment costs and longer break-even periods. Moreover, the shared PV-battery system shows greater sensitivity to variations in objective weights, suggesting coupling among system size, shared energy utilization, and economic performance at larger scales. The non-linear responses further suggest the existence of optimal operating regions where balanced trade-offs between cost, emission reduction, and energy autonomy can be achieved.

3.2 Comparative Assessment: Standalone and Shared PV-Battery Systems

This section examines the household-level resource and economic requirements associated with achieving different levels of PV reliance in standalone and shared systems. Fig. 5 shows the household-level variations in battery storage, panel area, lifetime cost, and payback period for both systems at different weight combinations. From the distribution shown in Fig. 5, approximately 98% of standalone system solutions achieve a reliability greater than 80%, whereas only about 85% of shared system solutions exceed this threshold. The lower fraction of high-reliance solutions in the shared system can arise from several interconnected technical and economic factors. The primary reason could be the substantially higher aggregate energy demand and temporal load variability at the community scale, where energy sharing improves load balancing and reduces redundant storage requirements, but also increases the total continuous energy requirements that the PV-battery infrastructure must meet. In this scenario, achieving high reliance requires larger PV-battery configurations, which is not optimal under the weighted multi-objective framework.

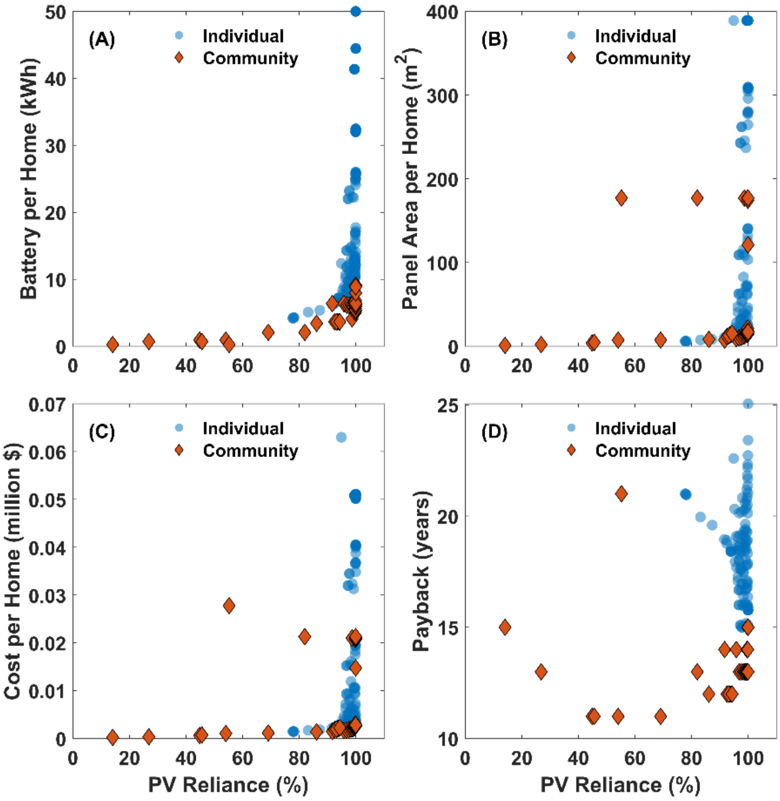

Figure 5. Per-home distribution of (A) battery storage, (B) panel area, (C) lifetime cost, and (D) payback period with PV reliance obtained for standalone and shared systems across all weight combinations.

The distribution shown in Fig. 5 demonstrates that shared system integration substantially reduces per-household resource and economic requirements needed to achieve high PV reliance (>80%) compared to standalone systems. Most prominently, the average battery storage requirements for a certain PV reliance decrease from 26 ± 13 kWh for individual-home systems to 6 ± 2 kWh for shared systems, corresponding to nearly a fourfold reduction. Similarly, the required panel area per home decreases from 254 ± 166 m^2 to 113 ± 79 m^2. These reductions indicate that shared energy and storage at the community level significantly improve infrastructure utilization efficiency by exploiting load diversity and reducing redundancy in system sizing, highlighting the potential benefits of future cooperative energy sharing practices.

The economic benefits are also pronounced, with lifetime cost per household decreasing from 0.034 ± 0.021 million USD for individual systems to 0.0143 ± 0.009 million USD for shared systems.

Additionally, the shared systems exhibit shorter, more consistent payback periods (12.96 ± 0.42 years) than the standalone systems (16.36 ± 2.08 years). These observations demonstrate that shared PV-battery infrastructure can substantially lower the financial burden of achieving high renewable energy penetration, while improving economic stability and reducing sensitivity to variations in system design. For all weight combinations, the percentage change in six metrics (panel area, battery storage, PV reliance, avoided CO_2 emissions, lifetime cost, and payback period) for community-scale systems relative to individual-home-level systems is presented in Table 2.

Table 2. Variations in panel area, battery storage, PV reliance, carbon mitigation potential, lifetime cost, and payback period for standalone and shared systems

	Metric	Panel Area (m^2)	Battery Storage (kWh)	PV Reliance (%)	CO_2 Mitigation (tonnes CO_2)	Lifetime Cost (x 10^4 USD)	Payback Period (years)
Mean ± Std	**Standalone (S)**	251 ± 168	26 ± 13	98 ± 5	54 ± 36	3.30 ± 2.13	16.42 ± 2.14
	Shared (SH)	98 ± 82	5 ± 2	90 ± 20	21 ± 18	1.20 ± 0.97	12.80 ± 0.95
	$\Delta\ (\%) = \mathbf{100}\dfrac{\boldsymbol{S-SH}}{\boldsymbol{S}}$	61 ± 42	81 ± 12	8 ± 21	61 ± 42	64 ± 38	22 ± 12

The comparative analysis presented here provides insights into the effect of energy sharing at the community scale on per-household infrastructure and economic burden required to achieve high renewable energy penetration. While these comparisons highlight the overall benefits of shared systems, the optimization outcomes remain strongly influenced by the interactions among multiple conflicting objectives and weighting combinations. Therefore, to further identify the dominant patterns governing the trade-offs between technical, environmental, and economic objectives, principal component analysis (PCA) is performed in the next section.

3.3 Principal Component Analysis of Multi-Objective Optimization Trade-Offs

PCA is a multivariate statistical technique used to reduce the dimensionality of complex datasets while retaining the dominant patterns and variability of the original variables [41,42]. PCA transforms a set of correlated variables into a smaller set of orthogonal variables, called principal components (PCs), which are linear combinations of the original variables. In this study, PCA is applied to identify the dominant patterns governing the trade-offs between technical and economic performance metrics. From the previous analysis, it is observed that the panel area directly governs the carbon mitigation potential; emissions have been excluded to avoid redundancy and artificial correlation effects. Therefore, PCA has been performed using percentage changes (listed in Table 2) across the panel area, battery storage, PV reliance, lifetime cost, and payback period. Prior to PCA, all variables are standardized using z-score normalization to ensure equal weighting regardless of scale [43].

Usually, the first few PCs collectively explain most of the variations in the solution space and therefore provide a compact representation of the multi-objective optimization landscape. To further identify the similarities among the solutions, k-means clustering [44] is applied in the reduced PCA space to identify primary clusters that represent distinct system behavior and trade-off patterns. Subsequently, the favorable solutions across all weight combinations are ranked and segregated based on an optimal score function formulated using normalized PCs. The formulation of the optimal score function, variable coefficients, and established relationships between different PCs and variables are discussed in Section S3. Fig. 6 demonstrates the distribution of the optimization solutions in the reduced PCA space defined by PC1, PC2, and PC3, along with the prominent clusters. The color distribution represents the optimal score, indicating the relative favorability of the solutions, while the cluster boundaries help identify groups of solutions with similar optimization behavior across different weight combinations.

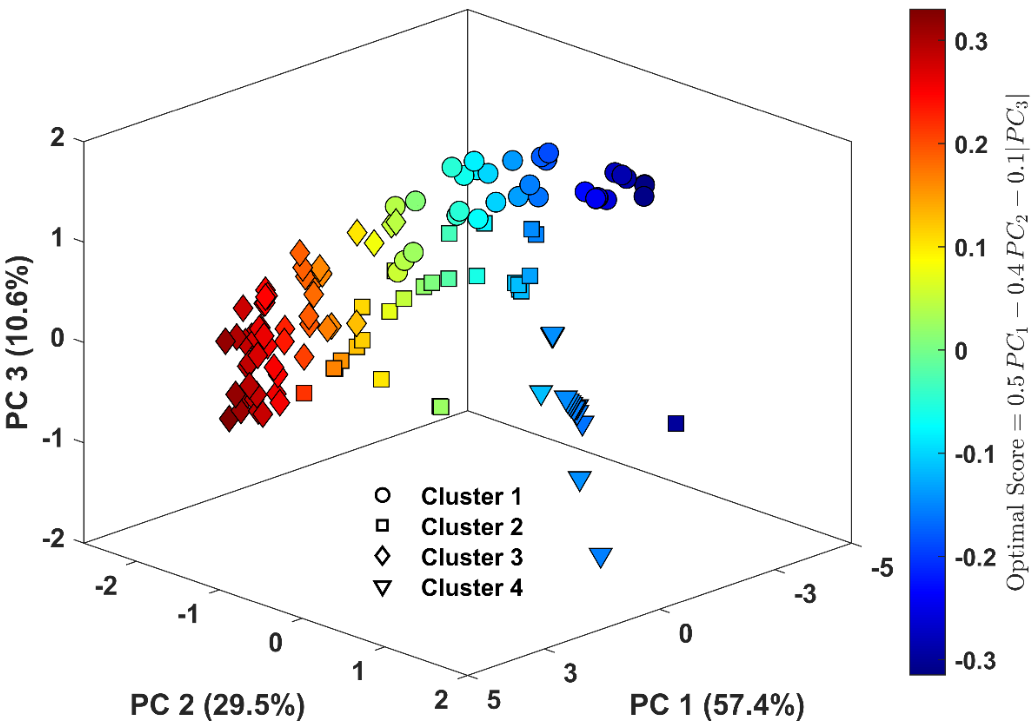

Figure 6. Principal component analysis (PCA) representation of the multi-objective optimization solutions in the reduced PC1-PC2-PC3 space, with clustering-based classification of the solutions and their corresponding optimal scores.

The PCA results reveal that the first three components (PC1: 57.4%, PC2: 29.5%, and PC3:10.6%) explain most of the variance, collectively accounting for 97.5% of the variability in the optimization space. This also indicates that these PCs sufficiently capture the dominant trends and trade-offs governing the multi-objective outcomes. The expression of PC1 and the coefficients of the independent variables (Eq. S2) indicate that the lifetime cost (0.561), panel area (0.557), and battery storage (0.457) account for the variation, highlighting that PC1 primarily reflects the infrastructure and system scale. Higher values of PC1 correspond to solutions requiring larger PV sizes and greater battery storage capacity, along with a larger economic investment to achieve higher energy autonomy. On the other hand, PC2 (Eq. S3) is strongly governed by the payback period (0.793) and PV reliance (0.484), with a moderate negative contribution from battery storage (-0.363). Solutions with higher PC2 values exhibit longer payback periods despite achieving higher PV reliance. The negative contribution of battery storage suggests that some solutions achieve reliance primarily through increased PV size rather than proportional storage expansion. Lastly, PC3 reflects a balancing behavior among competing objectives, with positive influence from PV reliance (0.564) and battery storage (0.555), and negative contributions from panel area (-0.450) and lifetime cost (-0.411). This indicates that PC3 differentiates between storage-heavy, high-reliability solutions from infrastructure-dependent, expensive configurations. Moreover, PC3 only explains a small fraction (10.6%) of the total variance, and it captures secondary trade-offs among the optimization objectives.

4. Conclusion

The present study systematically investigates the comparative performance of standalone and shared PV-battery systems under a multi-objective optimization framework. The analysis demonstrates that shared system integration substantially improves infrastructure utilization efficiency and economic feasibility relative to independently optimized household systems. Across all weight combinations, the shared system reduced per-household panel area requirements from 251 ± 168 m^2 to 98 ± 82 m^2, corresponding to a reduction of 61 ± 42 %. Similarly, battery storage requirements decreased from 26 ± 13 kWh to 5 ± 2 kWh, yielding an average reduction of 81± 12 %. These substantial reductions indicate that a distributed architecture and energy sharing can effectively exploit load diversity and shared energy storage, thereby reducing the degree of infrastructure oversizing required in individual-home systems. The weight-sensitivity analysis showed that aggressive minimization of lifetime cost generally leads to reductions in PV reliance and storage sizing, highlighting the inherent trade-offs between renewable-energy penetration and economic feasibility. Furthermore, a PCA-based framework has been developed to identify the dominant trade-offs governing the solution space. The first three principal components collectively explained approximately 97.5% of the total variance, demonstrating that the optimization behavior can be effectively represented in a reduced-dimensional space. The PCA revealed that the optimization landscape is primarily governed by infrastructure intensity, economic-return behavior, and secondary balancing trade-offs among storage, reliance, and cost.

Despite these insights, the present study has certain limitations. The analysis assumes deterministic load and solar-generation behavior, without explicitly accounting for uncertainties in weather variability, future electricity pricing, battery degradation dynamics, or demand-side behavioral changes. Future work should therefore focus on integrating uncertainty-aware optimization approaches, dynamic pricing mechanisms, stochastic renewable-energy generation, battery aging effects, and real-time energy-sharing strategies. Incorporation of peer-to-peer trading, grid flexibility services, and adaptive control frameworks could further improve the performance and economic viability of community-scale renewable-energy systems. Nevertheless, this study highlights the strong potential of integrating shared PV-battery systems as a practical pathway toward economically viable, infrastructure-efficient renewable-energy adoption for energy security and autonomy.

Acknowledgement

We acknowledge the funding provided by IIT Gandhinagar as a fellowship for Nishchaya Kumar Mishra to conduct this work. We also thank Dr. Venkatasailanathan Ramadesigan for his helpful feedback to carry out this work.

References

[1] Home | Statistical Review of World Energy n.d. https://www.energyinst.org/statistical-review (accessed February 5, 2025).

[2] Mishra NK, Patel S. Need for a Holistic Approach to Assessing Sustainable, Green, and Healthy Buildings. Environment & Health 2024. https://doi.org/10.1021/ENVHEALTH.4C00161.

[3] United Nations Environment Programme. Global Status Report for Buildings and Construction: Towards a Zero-emission, Efficient and Resilient Buildings and Construction Sector. Nairobi. 2022.

[4] International Energy Agency. World Energy Outlook 2023. 2023.

[5] Mishra NK, Vance ME, Novoselac A, Patel S. Dynamic optimization of personal exposure and energy consumption while ensuring thermal comfort in a test house. Build Environ 2024;252:111265. https://doi.org/10.1016/J.BUILDENV.2024.111265.

[6] Mishra NK, Batra N, Patel S. Optimizing Pollutant Exposure, Energy Consumption, and Thermal Comfort in a House via Deep Reinforcement Learning Control. Journal of Building Engineering 2025:114074. https://doi.org/10.1016/J.JOBE.2025.114074.

[7] Mishra NK, Patel S. From one building to many: transferability of a deep reinforcement learning agent for optimizing pollutant exposure and energy

consumption. Environmental Science: Advances 2026. https://doi.org/10.1039/D5VA00438A.

[8] D'Agostino D, Mazzarella L. What is a Nearly zero energy building? Overview, implementation and comparison of definitions. Journal of Building Engineering 2019;21:200–12. https://doi.org/10.1016/J.JOBE.2018.10.019.

[9] Brambilla A, Salvalai G, Imperadori M, Sesana MM. Nearly zero energy building renovation: From energy efficiency to environmental efficiency, a pilot case study. Energy Build 2018;166:271–83. https://doi.org/10.1016/J.ENBUILD.2018.02.002.

[10] Li H, Wang S. New challenges for optimal design of nearly/net zero energy buildings under post-occupancy performance-based design standards and a risk-benefit based solution Article History. Build Simul 2021;15:685–98. https://doi.org/10.1007/s12273-021-0857-9.

[11] Li SY, Han JY. The impact of shadow covering on the rooftop solar photovoltaic system for evaluating self-sufficiency rate in the concept of nearly zero energy building. Sustain Cities Soc 2022;80:103821. https://doi.org/10.1016/J.SCS.2022.103821.

[12] Jain M, Rawal R. Emissions from a net-zero building in India: life cycle assessment. Building & Cities 2022;3:398–416. https://doi.org/10.5334/bc.194.

[13] Li X, Lin A, Young CH, Dai Y, Wang CH. Energetic and economic evaluation of hybrid solar energy systems in a residential net-zero energy building. Appl Energy 2019;254:113709. https://doi.org/10.1016/J.APENERGY.2019.113709.

[14] Mishra NK, Biswas P, Patel S. Future of clean energy for cooking in India: A comprehensive analysis of fuel alternatives. Energy for Sustainable Development 2024;81:101500. https://doi.org/10.1016/J.ESD.2024.101500.

[15] Tantisattayakul T, Kanchanapiya P. Adoption, fiscal cost, and policy compromise: Evaluating residential rooftop solar policies in Thailand for emerging economies. Energy for Sustainable Development 2026;93:101986. https://doi.org/10.1016/J.ESD.2026.101986.

[16] Joshi S, Mittal S, Holloway P, Shukla PR, Ó Gallachóir B, Glynn J. High resolution global spatiotemporal assessment of rooftop solar photovoltaics potential for renewable electricity generation. Nature Communications 2021 12:1 2021;12:1–15. https://doi.org/10.1038/s41467-021-25720-2.

[17] Pablo-Romero M del P, Pozo-Barajas R, Yñiguez R. Global changes in residential energy consumption. Energy Policy 2017;101:342–52. https://doi.org/10.1016/J.ENPOL.2016.10.032.

[18] Electricity consumption – Electricity Information: Overview – Analysis - IEA n.d. https://www.iea.org/reports/electricity-information-overview/electricity-consumption (accessed February 5, 2025).

[19] Alipour M, Salim H, Stewart RA, Sahin O. Residential solar photovoltaic adoption behaviour: End-to-end review of theories, methods and approaches. Renew Energy 2021;170:471–86. https://doi.org/10.1016/J.RENENE.2021.01.128.

[20] Shakeel SR, Yousaf H, Irfan M, Rajala A. Solar PV adoption at household level: Insights based on a systematic literature review. Energy Strategy Reviews 2023;50:101178. https://doi.org/10.1016/J.ESR.2023.101178.

[21] Qureshi TM, Ullah K, Arentsen MJ. Factors responsible for solar PV adoption at household level: A case of Lahore, Pakistan. Renewable and Sustainable Energy Reviews 2017;78:754–63. https://doi.org/10.1016/J.RSER.2017.04.020.

[22] Konzen G, Best R, de Castro NJ. The energy injustice of household solar energy: A systematic review of distributional disparities in residential rooftop solar adoption. Energy Res Soc Sci 2024;111:103473. https://doi.org/10.1016/J.ERSS.2024.103473.

[23] Alsharif A, Almabsout E, Ahmed AA, Khaleel M, Nassar YF, El-Khozoadar HJ. Optimal Sizing of Hybrid Renewable System for Residential Appliances. 2024 IEEE 4th International Maghreb Meeting of the Conference on Sciences and Techniques of Automatic Control and Computer Engineering, MI-STA 2024 - Proceeding 2024:290–5. https://doi.org/10.1109/MI-STA61267.2024.10599729.

[24] Nematirad R, Pahwa A, Natarajan B. A Novel Statistical Framework for Optimal Sizing of Grid-Connected Photovoltaic–Battery Systems for Peak Demand Reduction to Flatten Daily Load Profiles. Solar 2024, Vol 4, Pages 179-208 2024;4:179–208. https://doi.org/10.3390/SOLAR4010008.

[25] Khanal S, Khezri R, Mahmoudi A, Kahourzadeh S. Effects of energy sharing and electricity tariffs on optimal sizing of PV-battery systems for grid-connected houses. Computers and Electrical Engineering 2024;118:109457. https://doi.org/10.1016/J.COMPELECENG.2024.109457.

[26] O'Shaughnessy E, Cutler D, Ardani K, Margolis R. Solar plus: Optimization of distributed solar PV through battery storage and dispatchable load in residential buildings. Appl Energy 2018;213:11–21. https://doi.org/10.1016/J.APENERGY.2017.12.118.

[27] Ritchie MJ, Avenant J, Engelbrecht JAA, Rix AJ, Booysen MJ. Optimal sizing of battery-less domestic rooftop PV systems in South Africa using a probabilistic electricity synthesiser. Energy for Sustainable Development 2023;76:101268. https://doi.org/10.1016/J.ESD.2023.101268.

[28] Okoye CO, Solyalı O. Optimal sizing of stand-alone photovoltaic systems in residential buildings. Energy 2017;126:573–84. https://doi.org/10.1016/J.ENERGY.2017.03.032.

[29] Vahabi Khah M, Zahedi R, Eskandarpanah R, Mirzaei AM, Farahani ON, Malek I, et al. Optimal sizing of residential photovoltaic and battery system connected to the power grid based on the cost of energy and peak load. Heliyon 2023;9:e14414. https://doi.org/10.1016/J.HELIYON.2023.E14414.

[30] Khawaja Y, Giaouris D, Patsios H, Dahidah M. Optimal cost-based model for sizing grid-connected PV and battery energy system. 2017 IEEE Jordan Conference on Applied Electrical Engineering and Computing Technologies, AEECT 2017 2017;2018-January:1–6. https://doi.org/10.1109/AEECT.2017.8257779.

[31] Qiu M, Zhu W, Feng S, Zhang Z. Assessment of rooftop photovoltaic potential in low-electrified rural areas of Zambia. Energy for Sustainable Development 2026;93:102028. https://doi.org/10.1016/J.ESD.2026.102028.

[32] Kang LW, Zhao X, Ma J. A new neural network model for the state-of-charge estimation in the battery degradation process. Appl Energy 2014;121:20–7. https://doi.org/10.1016/J.APENERGY.2014.01.066.

[33] O'Kane SEJ, Ai W, Madabattula G, Alonso-Alvarez D, Timms R, Sulzer V, et al. Lithium-ion battery degradation: how to model it. Physical Chemistry Chemical Physics 2022;24:7909–22. https://doi.org/10.1039/D2CP00417H.

[34] Luo G, Zhang Y, Tang A. Capacity Degradation and Aging Mechanisms Evolution of Lithium-Ion Batteries under Different Operation Conditions. Energies (Basel) 2023;16:4232. https://doi.org/10.3390/EN16104232/S1.

[35] Wildfeuer L, Karger A, Aygül D, Wassiliadis N, Jossen A, Lienkamp M. Experimental degradation study of a commercial lithium-ion battery. J Power Sources 2023;560:232498. https://doi.org/10.1016/J.JPOWSOUR.2022.232498.

[36] Xu B, Oudalov A, Ulbig A, Andersson G, Kirschen DS. Modeling of lithium-ion battery degradation for cell life assessment. IEEE Trans Smart Grid 2018;9:1131–40. https://doi.org/10.1109/TSG.2016.2578950.

[37] IEX | Indian Energy Exchange n.d. https://www.iexindia.com/ (accessed February 8, 2025).

[38] India's Power Sector | Capacity & Generation Mix n.d. https://iced.niti.gov.in/energy/electricity/generation (accessed February 6, 2025).

[39] CDM - CO2 Baseline Database - Central Electricity Authority n.d. https://cea.nic.in/cdm-co2-baseline-database/?lang=en (accessed February 6, 2025).

[40] General Review Report - Central Electricity Authority n.d. https://cea.nic.in/general-review-report/?lang=en (accessed February 6, 2025).

[41] Jollife IT, Cadima J. Principal component analysis: a review and recent developments. Philos Trans A Math Phys Eng Sci 2016;374:20150202. https://doi.org/10.1098/RSTA.2015.0202.

[42] Greenacre M, Groenen PJF, Hastie T, D'Enza AI, Markos A, Tuzhilina E. Principal component analysis. Nature Reviews Methods Primers 2022 2:1 2022;2:100-. https://doi.org/10.1038/s43586-022-00184-w.

[43] Score Normalization - an overview | ScienceDirect Topics n.d. https://www.sciencedirect.com/topics/computer-science/score-normalization (accessed May 9, 2026).

[44] Ikotun AM, Ezugwu AE, Abualigah L, Abuhaija B, Heming J. K-means clustering algorithms: A comprehensive review, variants analysis, and advances in the era of big data. Inf Sci (N Y) 2023;622:178–210. https://doi.org/10.1016/J.INS.2022.11.139.